A new PWM control method for AC to DC converters with high-frequency transformer isolation

A New PWM Control Method for ac to dc Converters with High-Frequency Transformer Isolation

Katsuhisa Inagaki, Takeshi Furuhashi, Akio Ishiguro, Muneaki
Ishida, *Member, IEEE*, and Shigeru Okuma, *Member, IEEE*

Abstract—This paper presents a novel PWM control method for a switch mode rectifier (SMR) based on the idea of coordinate transformation. The proposed method realizes sinusoidal input current waveforms, a controllable input displacement factor, and an arbitrary output voltage waveform. This method is suitable for real-time control.

Simulations and experiments are carried out to confirm feasibility of the proposed method.

I. INTRODUCTION

TRANSFORMER isolation is a usual practice for ohmic isolation between a source and a load. The transformer designed for commercial frequency makes the converter bulky and heavy. Therefore, high-frequency link converters have been studied minimize weight, size, and cost of the converters by making the transformer smaller [1]–[3].

Manias and Ziogas proposed a novel switch-mode-rectifier (SMR) structure and showed a control method [4]. The structure having six force-commutated switches with bidirectional current flow is simpler than those of the conventional ac-dc high-frequency dc-type converters. The control method proposed in [4], which is a combination of the control method of PWM converters and that of PWM inverters, makes the input power factor controllable and reduces the harmonics in the input current. However, the method in [4] still generates lots of harmonics in the input current and does not seem adequate for real-time control of arbitrary output voltage waveforms.

In this paper, a novel PWM control method for the SMR derived from the idea of coordinate transformation [5] is proposed. The proposed method realizes sinusoidal input current waveforms, controllable input displacement factor, and arbitrary output voltage waveforms. Moreover, this method is advantageous to reduce higher and fractional harmonic components of the input waveforms than the previous method and is more suitable for real-time control. Suppression of dc magnetization of the high-frequency transformer is easy to implement.
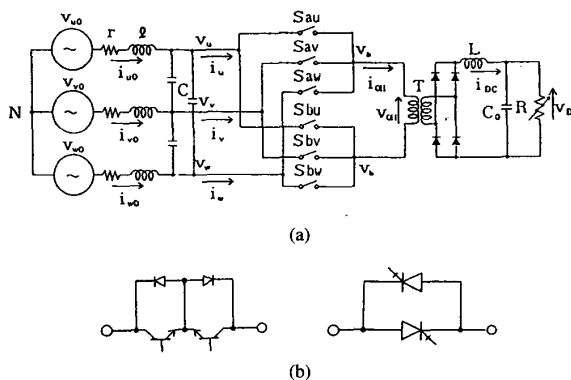
Fig. 1. Switch mode rectifier: (a) Main circuit; (b) practical switching device.

Simulations and experiments are carried out to confirm feasibility of the proposed method.

II. MAIN CIRCUIT

The main circuit of the SMR is shown in Fig. 1(a), which consist of six self-turn-off bidirectional switches S_{au}–S_{bw}, input l-C-r filters, a high-frequency transformer T, a diode bridge, and a L-C_o filter. The ohmic isolation between the source and the load is realized by the high-frequency transformer. Practical bidirectional switches for S_{au}–S_{bw} are shown in Fig. 1(b). Each switch consists of two self-turn-off devices with reverse blocking capability. The efficiency of the SMR is to be improved by using GTO's. The GTO's reduce the number of devices connected in series in the operation of the SMR. The input l-C-r filters are used to eliminate high-frequency components in the input current of the SMR. The inductance of the source line is included in the filter reactor l, and the resistor r is a sum of the resistor of the reactor and that of the source line. The filter L-C_o suppresses the high frequency components of the output voltage of the SMR.

The source voltages v_{uo}, v_{vo}, v_{wo} and the voltages after the input l-C-r filters v_u, v_v, v_w are given as the following expressions:

$$\begin{bmatrix} v_{uo} \\ v_{vo} \\ v_{wo} \end{bmatrix} = Vs \begin{bmatrix} \cos \omega t \\ \cos(\omega t - 2\pi/3) \\ \cos(\omega t + 2\pi/3) \end{bmatrix} \quad (1)$$

$$\begin{bmatrix} v_u \\ v_v \\ v_w \end{bmatrix} = V \begin{bmatrix} \cos(\omega t - \delta) \\ \cos(\omega t - \delta - 2\pi/3) \\ \cos(\omega t - \delta + 2\pi/3) \end{bmatrix} \quad (2)$$
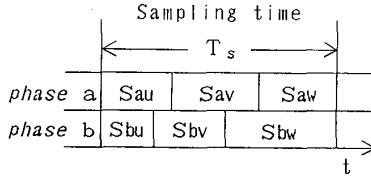
Fig. 2. Switching pattern.

where ω is the angular frequency of the source, V_s is the amplitude of the source voltages, V is the amplitude of the voltages after the input *l-C-r* filters, and δ is the phase lag caused by the input *l-C-r* filters.

III. CONTROL FUNCTIONS

Since the filter capacitor C's are connected on the source side of the bidirectional switches Sau-Sbw, short-circuit of the capacitors by the switches is not allowed. Since the high-frequency transformer with a leakage inductance is connected on the output side of the switches, the open circuit of the output terminals is not favorable. Therefore, the switches Sau-Sbw are controlled as shown in Fig. 2. For real-time control, switching patterns are generated at every sampling period T_s. A control function for each switch is defined as a duty ratio within each T_s and is denoted by $a_u - b_w$. For instance, a_u is defined as follows:

$$a_u = (\text{on-time of } Sau \text{ during } T_s)/T_s. \tag{3}$$

The following constraints are imposed on the control functions:

$$\begin{aligned} a_u + a_v + a_w &= 1 \\ b_u + b_v + b_w &= 1 \end{aligned} \tag{4}$$

where

$$0 < a_q < 1, \quad 0 < b_q < 1 \, (q = u, \, v, \, w).$$

The voltages on the primary side of the high-frequency transformer are denoted by v_a and v_b. These voltages are viewed from the neutral point N. The average values of the voltages v_a, v_b during the sampling period T_s are given as follows:

$$\begin{bmatrix} \overline{v_a} \\ \overline{v_b} \end{bmatrix} = \begin{bmatrix} a_u & a_v & a_w \\ b_u & b_v & b_w \end{bmatrix} \begin{bmatrix} v_u \\ v_v \\ v_w \end{bmatrix}. \tag{5}$$

The input currents are denoted by i_u, i_v, i_w. The average value of the input currents during the sampling period $\overline{i_u}, \overline{i_v}, \overline{i_w}$, are given by using the current of the primary winding of the high-frequency transformer i_{OH} as:

$$\begin{bmatrix} \overline{i_u} \\ \overline{i_v} \\ \overline{i_w} \end{bmatrix} = \begin{bmatrix} a_u & b_u \\ a_v & b_v \\ a_w & b_w \end{bmatrix} \begin{bmatrix} i_{OH} \\ -i_{OH} \end{bmatrix}. \tag{6}$$

We propose the following control functions based on the idea of coordinate transformation [5]:

$$\begin{bmatrix} a_u \\ a_v \\ a_w \end{bmatrix} = A_v Y_a \begin{bmatrix} X_u \\ X_v \\ X_w \end{bmatrix} + \begin{bmatrix} h_u \\ h_v \\ h_w \end{bmatrix}$$

$$\begin{bmatrix} b_u \\ b_v \\ b_w \end{bmatrix} = A_v Y_b \begin{bmatrix} X_u \\ X_v \\ X_w \end{bmatrix} + \begin{bmatrix} h_u \\ h_v \\ h_w \end{bmatrix} \tag{7}$$

where A_v determines the amplitude of the output voltage on the primary side of the high-frequency transformer. Functions h_u, h_v, h_w are introduced to satisfy the constraints in (4). X_u, X_v, and X_w are given as follows:

$$\begin{bmatrix} X_u \\ X_v \\ X_w \end{bmatrix} = \begin{bmatrix} \cos(\omega t + \phi_s) \\ \cos(\omega t + \phi_s - 2\pi/3) \\ \cos(\omega t + \phi_s + 2\pi/3) \end{bmatrix} \tag{8}$$

where ϕ_s is the demand of the phase difference between the input voltages, V_u, V_v, V_w an the input currents i_u, i_v, i_w. By substituting (2), (7), and (8) into (5), the average values of the voltages during the sampling period $\overline{v_a}, \overline{v_b}$ are obtained as follows:

$$\begin{bmatrix} \overline{v_a} \\ \overline{v_b} \end{bmatrix} = \frac{3}{2} A_v V \cos(\phi_s + \delta) \begin{bmatrix} Y_a \\ Y_b \end{bmatrix} + \begin{bmatrix} v_0 \\ v_0 \end{bmatrix} \tag{9}$$

where v_0 is expressed as:

$$v_0 = h_u V_u + h_v V_v + h_w V_w. \tag{10}$$

Then, the average value of the voltage across the primary winding of the high-frequency transformer during the sampling period $\overline{v_{OH}}$ is obtained as

$$\overline{v_{OH}} = \overline{v_a} - \overline{v_b} = \frac{3}{2} A_v V \cos(\phi_s + \delta)(Y_a - Y_b). \tag{11}$$

Functions Y_a and Y_b in (7) and (11) appear across the primary winding of the high-frequency transformer. These functions determine the waveform of the voltage v_{OH}. The output dc voltage V_{DC} is obtained by rectifying the smoothing the voltage v_{OH}. Therefore, the output dc voltage V_{DC} can be controlled by the value A_v. The output voltage generated by the functions h_u, h_v, h_w is a zero-phase component and does not appear across the primary winding of the high-frequency transformer.

The functions Y_a and Y_b can be any kind of waveforms. To realize the least switching frequency of the switches Sau-Sbw under the link frequency ω_0, the functions are chosen as

$$\begin{bmatrix} Y_a \\ Y_b \end{bmatrix} = \begin{bmatrix} \text{sgn}(\sin \omega_0 t) \\ \text{sgn}(-\sin \omega_0 t) \end{bmatrix}. \tag{12}$$

Assuming that the dc output current i_{DC} does not contain ripple component (i.e., $i_{DC} = I$ (constant)), the primary current of the high-frequency transformer i_{OH} is expressed as

$$i_{OH} = I(Y_a - Y_b/2). \tag{13}$$

The average value of the input current during the sampling period $\overline{i_u}, \overline{i_v}, \overline{i_w}$ are obtained by substituting (7), (8), (12), and (13) and (6).

$$\begin{bmatrix} \overline{i_u} \\ \overline{i_v} \\ \overline{i_w} \end{bmatrix} = A_v I \begin{bmatrix} X_u \\ X_v \\ X_w \end{bmatrix} = A_v I \begin{bmatrix} \cos(\omega t + \phi_s) \\ \cos(\omega t + \phi_s - 2\pi/3) \\ \cos(\omega t + \phi_s + 2\pi/3) \end{bmatrix}. \tag{14}$$

The input currents are sinusoidal. ϕ_s is the value introduced in (8) and determines the displacement factor of the input current.

TABLE I
EXAMPLE OF h_u, h_v, h_w AND SWITCHING SEQUENCE

MODE	1	2	3	4	5	6
X_u	+	+	−	−	−	+
X_v	−	+	+	+	−	−
X_w	−	−	−	+	+	+
h_u	$1-A_U \cdot X_u \cdot maxY_0$	$-A_U \cdot X_u \cdot minY_0$	$-A_U \cdot X_u \cdot maxY_0$	$1-A_U \cdot X_u \cdot minY_0$	$-A_U \cdot X_u \cdot maxY_0$	$-A_U \cdot X_u \cdot minY_0$
h_v	$-A_U \cdot X_v \cdot maxY_0$	$-A_U \cdot X_v \cdot minY_0$	$-A_U \cdot X_v \cdot maxY_0$	$-A_U \cdot X_v \cdot minY_0$	$-A_U \cdot X_v \cdot maxY_0$	$1-A_U \cdot X_v \cdot minY_0$
h_w	$-A_U \cdot X_w \cdot maxY_0$	$1-A_U \cdot X_w \cdot minY_0$	$1-A_U \cdot X_w \cdot maxY_0$	$-A_U \cdot X_w \cdot minY_0$	$1-A_U \cdot X_w \cdot maxY_0$	$-A_U \cdot X_w \cdot minY_0$
SWITCHING SEQUENCE	u → v → w	w → u → v	v → w → u	u → v → w	w → u → v	v → w → u

IV. FUNCTIONS h_u, h_v, h_w, AND THE MAXIMUM OUTPUT VOLTAGE

The functions h_u, h_v, h_w are derived from (4) and (7) as follows:

$$-A_v X_q \min Y_p < h_q < 1 - A_v X_q \max Y_p \quad (X_q > 0)$$
$$-A_v X_q \min Y_p < h_q < 1 - A_v X_q \min Y_p \quad (X_q > 0)$$
$$(q=u,v,w) \quad (15)$$

where

$$\min Y_p = \min(Y_a, Y_b)$$
$$\min Y_p = \min(Y_a, Y_b).$$

In addition, (4) and (7)

$$h_u + h_v + h_w = 0. \quad (16)$$

Assuming that the absolute value of X_w is the largest among those of the functions X_u, X_v, X_w is negative in a sampling period, and $Y_a = 1$, $Y_b = -1$. Then, the switching frequency is reduced by keeping the switch Sbw on, switches Sbu, Sbv off, and by controlling the output voltage with the switches Sau, Sav, Saw, as illustrated in Fig. 3. A sampling period in which $|X_w|$ is maximum is expanded in Fig. 3(b). The voltage across the primary winding of the high-frequency transformer v_{OH} consists of three waveforms in the sampling period. These waveforms are 1) zero voltage short circuited by the switches Saw and Sbw, 2) line-to-line voltage v_{uw} (Sau and Sbw on), and 3) line-to-line voltage v_{vw} (Sav and Sbw on). There is a freedom in the sequence of 1), 2), and 3). An example of h_u, h_v, h_w, and a switching sequence is listed in Table I. There are six modes depending on the maximum value of $|X_u|$, $|X_v|$, $|X_w|$. The switching sequence is denoted by the subscripts of the switches to be turned on/off in the mode. For example, Fig. 3 is the case of mode 2. The switches Sau, Sav, and Saw are turned on/off in the case; thus, the switching sequence is w-u-v. The distortion of the input currents of the SMR is reduced by the sequence in Table I [5].

Using the functions Y_a and Y_b of (12), the control functions of the switches $a_u \sim b_w$ are determined for each mode. For example, in mode 1
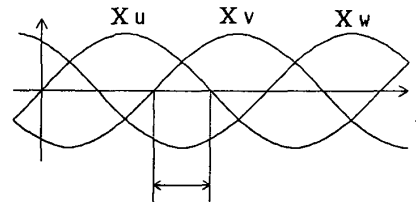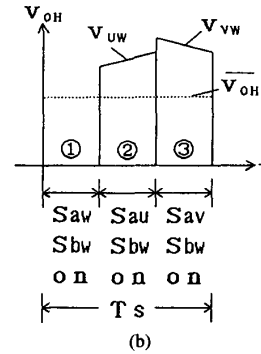
Fig. 3. Examples of (a) input functions (b) construction of output voltage.

if $Y_a = 1$ and $Y_b = -1$
$$a_u = 1$$
$$a_v = 0$$
$$a_w = 0$$
$$b_u = 1 - b_v - b_w$$
$$b_v = -2A_v X_v$$
$$b_w = -2A_v X_w$$
and
if $Y_a = -1$ and $Y_b = 1$
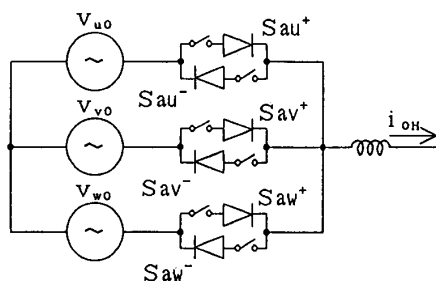$$a_u = 1 - a_v - a_w$$
$$a_v = -2A_v X_v$$

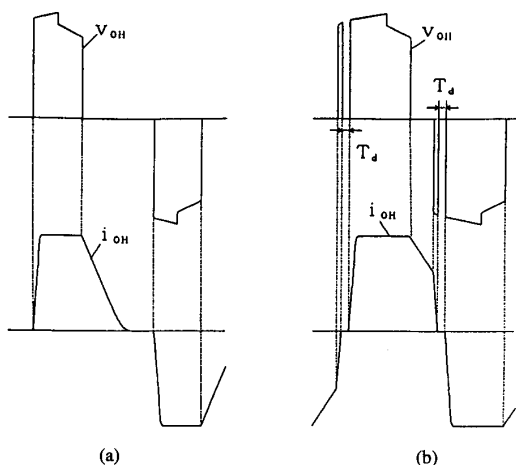Fig. 4. Equivalent circuit of an a phase of SMR.

Fig. 5. Waveforms of voltages and currents of primary winding of high-frequency transformer.
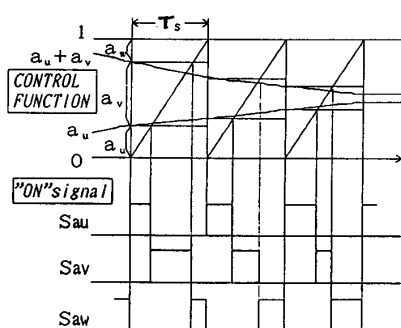

Fig. 6. Generation method of switching patterns.

$$a_w = -2A_v X_w$$
$$b_u = 1$$
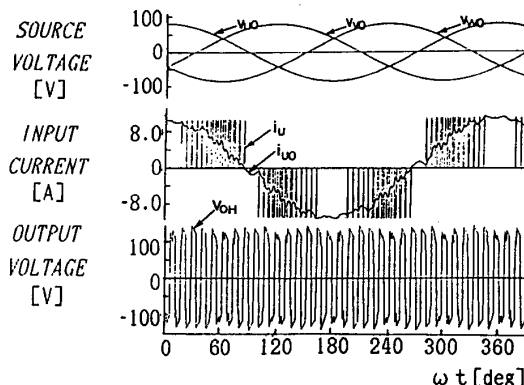$$b_v = 0$$
$$b_w = 0. \tag{17}$$

The control functions obtained above are simple. In the case that $\phi_s = 0$, the functions X_u, X_v, X_w are in phase with the input voltage v_u, v_v, v_w. It is found that on times of the switches Sav/Sbv and Saw/Sbw are in proportion to the absolute value of the input line-to-neutral voltage V_v and V_w in mode 1, respectively. As for the u phase, the
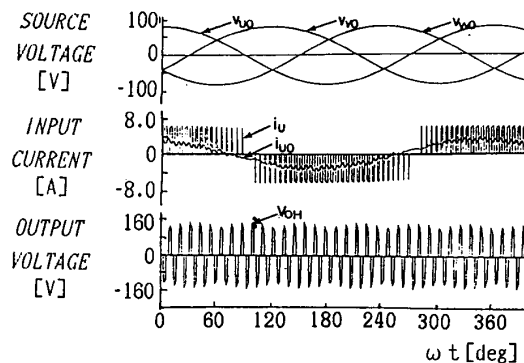
(a)
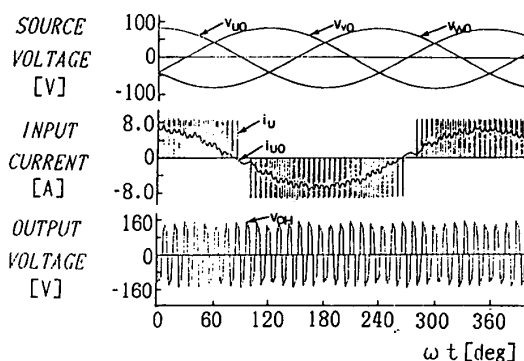
(b)

(c)

Fig. 7. Simulation results: (a) $A = 1/4$; (b) $A = 3/8$; (c) $A = 1/2$.

switches Sau/Sbu are kept on in mode 1. Since the output dc current i_{DC} is constant, the resulting input currents i_u, i_v, i_w, respectively.

The range of the function A_v in which the average value of the output voltage during the sampling period v_{OH} is kept constant in every sampling period is

$$0 < A_v < 1/2. \tag{18}$$

the maximum value of the voltage v_{OH} is derived from (11) as $(3/2) V \cos (\phi_s + \delta)$. If $\phi_s = 0$ and $V \cos \delta = V_s$, then the output voltage V_{CH} is 1.5 times as much as the amplitude of the line-to-neutral voltage V.
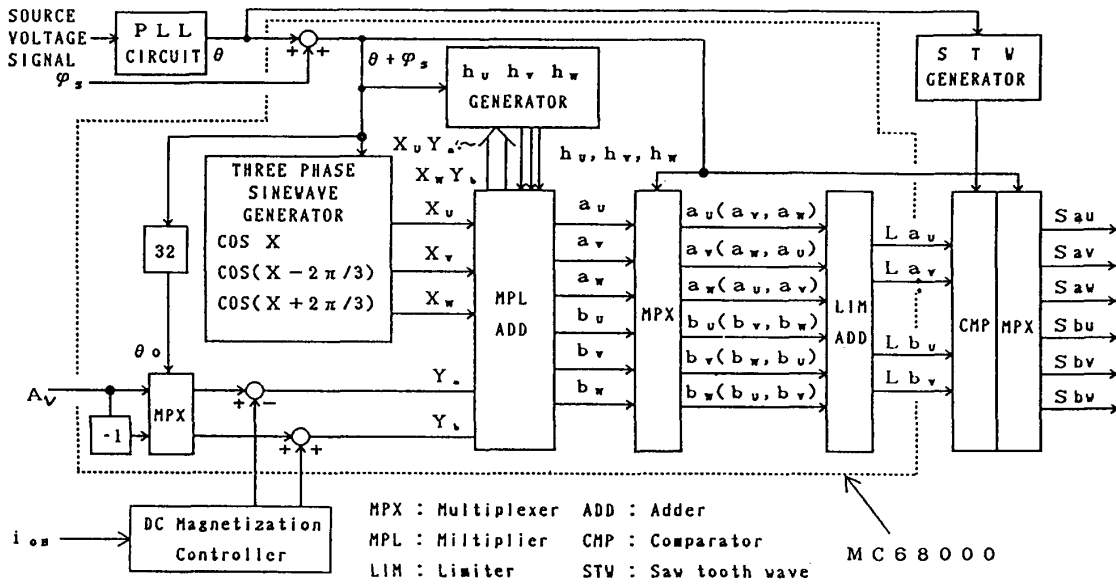
Fig. 8.   Block diagram of control circuit.

V. SUPPRESSION OF DC MAGNETIZATION OF HIGH-FREQUENCY TRANSFORMER

A dead time T_d is introduced against the short-circuit of the input filter capacitor C. Figure 4 shows an equivalent circuit with two reverse blocking self-turn-off devices for each switch. Assuming that $v_{uo} > v_{vo}$ and $i_{OH} < 0$, i_{OH} goes to the opposite sign at the time of commutation from Sav^- to Sau^-. If no dead time is set, Sau^+ is to be turned on, whereas the switch Sav^- is still in the on state. A small dead time is effective against the short circuit.

Fig. 5 shows examples of the voltage across the primary winding of the high-frequency transformer v_{OH} and the current of the primary winding of the transformer i_{OH}. Fig. 5(a) shows the case that the demand of the output voltage is small. The current i_{CH} goes to zero in the period of the zero-voltage output. In Fig. 5(b), the demand of the output voltage is large. The period of zero-voltage output is short, and the current i_{OH} has a certain amount when the voltage of opposite sign is generated. Then, the output voltage has a dip caused by the dead time. If dc component is contained in the output current, the dip may appear in the output voltage of only one polarity. In this case, the voltage drop causes positive feedback, and the dc component is increased. Then, the dc magnetization of the high-frequency transformer is aggravated.

This dc magnetization can easily be suppressed by detecting the dc component of the output current and by modifying the functions Y_a and Y_b properly.

VI. SIMULATIONS

Fig. 6 shows a generating method of the on signal of the switches Sau-Sbw. The control functions a_u and $a_u + a_w$ are sampled and held during the sampling period T_s. These functions are compared with a sawtooth waveform
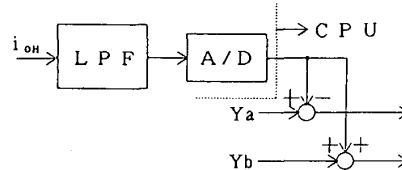

Fig. 9.   Circuit for dc demagnetization.

synchronized with the sampling time, and the on signals of Sau-Saw are generated. The on signals of Sbu-Sbw are generated using the control functions b_u and $b_u + b_v$. The switching sequence is u-v-w in this case. The switching sequence can be changed by the control functions to be sampled and held. For example, the switching sequence is v-w-u with the control functions of a_v and $a_v + a_w$.

Fig. 7 shows simulation results with (a) $A_v = 1/4$, (b) $A_v = 3/8$, and (c) $A_v = 1/2$. The sampling period is set at 1/64 of the period of the source voltage. Then, the frequency of the high-frequency link is 32 times as much as the source frequency (i.e., 60 Hz×32 = 1.92 kHz). Simulation conditions are listed in Table I. The capacitor on the dc side $C_{\overline{\sigma}}$ is large enough to absorb the switching ripple of the dc voltage. The switches are ideal, and no dead time is set. The input currents i_{uo} in Fig. 7 are nearly sinusoidal. The phases of input current i_{uo} lead to the source voltage v_{uo} due to the input filter capacitor C. The average value of the voltage across the primary winding of the high-frequency transformer is constant in every sampling period.

VII. EXPERIMENTS

Fig. 8 shows the block diagram of the controller. The electrical angle of the source voltage is obtained by the PLL circuit. Functions X_u, X_v, X_w are generated with ω and ϕ_s
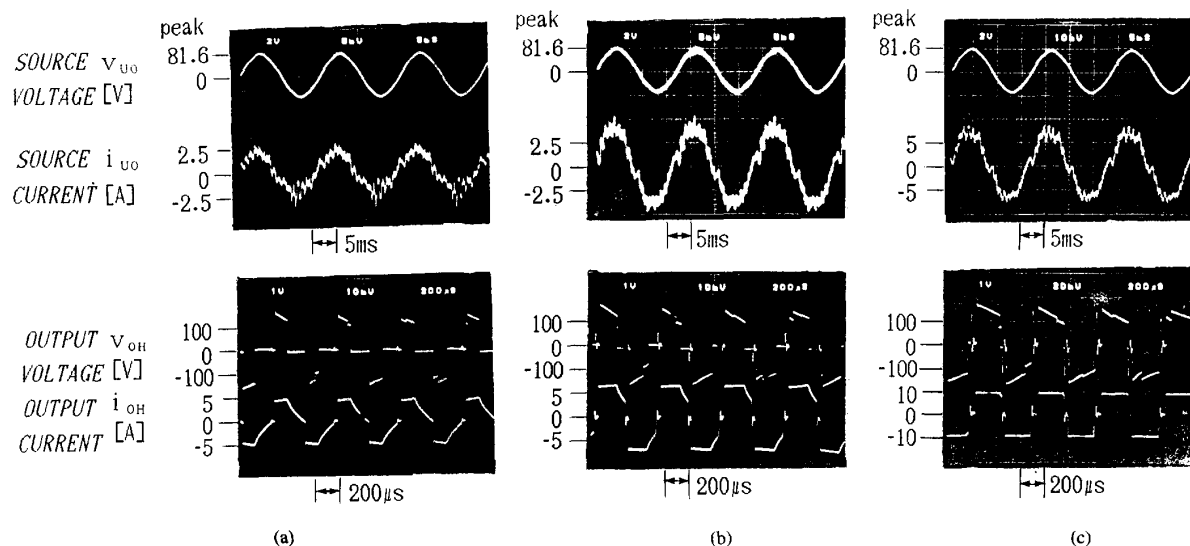
Fig. 10. Experimental results: (a) $A = 1/4$; (b) $A = 3/8$; (c) $A = 1/2$.

using a table. The electrical angle of the output voltage ω_o is obtained as $32(\omega_t + \phi_s)$. Functions Y_a and Y_b are generated by using the demand of the output dc voltage A_v and the ω_o. Functions h_u, h_v, h_w are generated by using Table I. The limitter works in case that the control functions $a_u - b_w$ do not satisfy the constraints in (4). The on-signals of Sau-Sbw are obtained by comparing La_u-Lb_v with the sawtooth wave. The portion enclosed by the broken line is realized with a microprocessor MC68000.

Fig. 9 show the circuit for suppressing the dc magnetization of the high-frequency transformer. The dc component is detected by a Hall sensor and a low-pass filter, and then, the functions Y_a and Y_b are modified.

Experimental results are shown in Fig. 10. Two bipolar transistors and two diodes are used as a bidirectional switch as shown in Fig. 1(b). The voltage demand A_v is 1/4 (Fig. 10(a)), 3/8 (Fig. 10(b)), and 1/2 (Fig. 10(c)). Other conditions are the same as those in the simulations. The dead time T_d for preventing the short circuit of the input filter capacitor is set at 20 μs. The ripples in the input current iuo are larger than those in the simulations. The large ripples are caused by the dead time. The obtained dc output voltages are a little bit smaller than the demands. This difference is mainly due to the dead time and the high-frequency transformer, which is not suitable for high-frequency use.

VIII. CONCLUSIONS

This paper presented a new control method for the SMR. The new method is based on the idea of coordinate transformation. Results are as follows:

1) The proposed method realized sinusoidal input current, an arbitrary output voltage waveform, and a controlable input displacement factor. The maximum input-to-output voltage ratio was 3/2.

2) The proposed method was suitable for real-time control of the voltage on the primary side of the high-frequency transformer. Thus, the suppression of the dc magnetization of the high-frequency transformer was easy to implement. Control of the output dc voltage was also easy.

3) Feasibility of the proposed method was confirmed by simulations and experiments.

REFERENCES

[1] P. H. Walter, "Forward converter operating directly off the three-phase rectified mains suitable for exchange use," in *Proc. Intelec 81*.
[2] S. A. Rosenberg *et al.*, "A new family of switched mode rectifiers," in *Proc. Intelec 81*.
[3] M. F. Schlecht, "Novel topological alternatives to the design of a harmonic-free utility/dc interface," in *Proc. IEEE Power Electron. Spec. Conf.*, 1983, p. 206.
[4] S. Manias and P. D. Ziogas, "A novel sinewave in ac to dc converter with high-frequency transformer isolation," *IEEE Trans. Ind. Electron.*, vol. IE-32, p. 430, 1985.
[5] A. Ishiguro *et al.*, "A new method of PWM control for forced commutated cycloconverters using microprocessors," *IEEE/IAS Conf. Rec.*, 1988, p. 712.
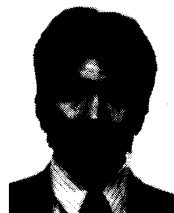
Katsuhisa Inagaki was born in Aichi, Japan, in 1965. He received the B.S. and M.S. degrees in 1988 and 1990 from Nagoya University, respectively, all in electrical and electronic engineering. He received the Ph.D. degree from Nagoya University in 1993.

Since 1990, he has been with Toshiba Cooperation, and he is in the doctoral program at Nagoya University. He is engaged in research on power electronics.
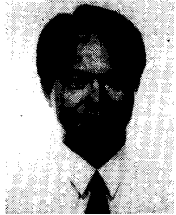
Dr. Inagaki is a member of the Institute of Electrical Engineers of Japan.

Akio Ishiguro was born in Kochi, Japan, on May 18, 1964. He received the B.S., M.S., and Ph.D. degrees in electronic-mechanical engineering form Nagoya University, Japan, in 1987, and 1989, and 1991, respectively.

Since 1991, he has been with the Department of Electronic-Mechanical Engineering of Nagoya University as an Assistant Professor. He is engaged in research on robotics, neural networks, and inverse problems.

Dr. Ishiguro is a member of the Institute of Electrical Engineers of Japan, the Society of Instrument and Control Engineers of Japan, the Institute of Electronics, Information, and Communication Engineers, and the Robotics Society of Japan.
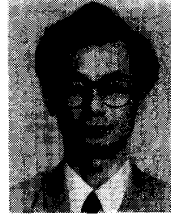
Muneaki Ishida (M'82) was born in Auchi, Japan, in 1952. He received the B.S., M.S., and Ph.D. degrees from Nagoya University, Japan, in 1975, 1977 and 1980, respectively, all in electrical and electronic engineering.

He was with Nagoya University as a Research Associate in the Department of Electrical Engineering from 1980 to 1987. Since 1987, he as been with Mie University, Tsu, Japan, as an Associate Professor. He is engaged in research on static power converters, induction motor drive systems, and the development of new motors using piezoelectric devices.

Dr. Ishida is a member of the IEEE IE, IA, AC, and UFFC Societies.

Takeshi Furuhashi was born in Shizuoka, Japan, in 1954. He received the B.E., M.E., and Ph.D. degrees in electrical engineering form Nagoya University, Japan, in 1980, 1982 and 1985, respectively.

He was with Toshiba Cooperation from 1985 to 1988. From 1988 to 1990, he was with Nagoya University as an Assistant Professor in the Department of Electrical Engineering. Since 1990, he has been an Associate Professor of the Department of Electronic-Mechanical Engineering of Nagoya University. His research interests are in fuzzy theory, neural networks and knowledge acquisition in AI.

Dr. Furuhashi is a member of the Institute of Electrical Engineers of Japan, the Society of Instrument and Control Engineers of Japan, and the Japan Society for Fuzzy Theory and Systems.

Shigeru Okuma (M'82) was born in Gifu, Japan, in 1948. He received the B.E., M.E., and Ph.D. degrees in electrical engineering from Nagoya University, Nagoya, Japan, in 1970, 1972, and 1978, respectively. He also received the M.E. degree in systems engineering from Case Western Reserve University, Cleveland, OH, in 1974.

From 1977 to 1984, he was with the Department of Electrical Engineering of Nagoya University. From 1985 to 1990, he was with the Department of Electronic-Mechanical Engineering of Nagoya University as an Associate Professor. Since 1990, he has been a Professor of the Department of Electronic-Mechanical Engineering of Nagoya University. His research interests are in the areas of power electronics, robotics, and micro/nano technology.

Dr. Okuma is a member of the Institute of Electrical Engineers of Japan, the Society of Instrument and Control Engineers of Japan, and the Robotics Society of Japan.